Cavity resonances in finite plasmonic chains

P. Ghenuche,[a] I. G. Cormack, G. Badenes, P. Loza-Alvarez, and R. Quidant[b]
ICFO-Institut de Ciencies Fotoniques, 08860 Castelldefels (Barcelona), Spain

(Received 27 September 2006; accepted 19 December 2006; published online 24 January 2007)

The authors report on the observation of cavity resonances along finite gold nanoparticle chains which, unlike continuous gold nanowires, lead to a high field concentration at their extremity. The mode signature has been assessed by probing the local field bound to the metal with two-photon luminescence spectroscopy. Simulations based on the Green dyadic method corroborate a good agreement with the measurements and bring further insight to the physics involved. © *2007 American Institute of Physics*. [DOI: 10.1063/1.2435513]

The elaboration of future nanophotonic devices relies on the optimization of light interaction with very small quantities of matter, down to the molecular level. For this purpose, much effort has been made to achieve high field intensity within small volumes. Resonant plasmon nanostructures promise a considerable potential for subwavelength light confinement through the creation of very strong surface charge gradients in the gap of dimers,[1] self-similar chains,[2] or at the apex of sharp metal tips.[3] Lately, Ditlbacher *et al.* have reported Fabry-Pérot cavity modes along 80 nm cross-section crystalline silver wires.[4] A similar behavior has been observed along a metal/dielectric/metal geometry.[5]

Here our attention focuses on periodic one-dimensional arrangements of noble metal nanoparticles lying onto a glass substrate. Such a configuration has recently increased interest for its ability to confine[6] and guide light through subwavelength cross sections.[7,8] In a previous study, we numerically identified peculiar resonances occurring for finite chains of closely spaced gold particles when illuminated under total internal reflection. These resonances were found to be associated with a strong local field enhancement at the chain output extremity.[9] In this letter, we report on the experimental observation by two-photon luminescence (TPL) spectroscopy of these resonances. Simulations based on the Green dyadic method corroborate a good agreement with our measurements and bring further insight in the physics involved.

The gold nanoparticle chains were fabricated by e-beam lithography on indium tin oxide coated glass substrates. Each sample contains several periodic arrays ($50\times 50\ \mu m^2$) of chains with different lengths, up to 20 particles. The gold particles forming the chains have a roughly cylindrical shape with an average diameter of 90 nm, 15 nm height, and spaced by 25 nm [Fig. 1(a)]. The separation distance between two adjacent chains was fixed to 1 μm to maximize the signal of the ensemble without significantly interfering with the near-field coupling between consecutive particles within each chain.

In our optical configuration, sketched in Fig. 1(b), the fabricated sample is optically connected to a hemicylindrical glass prism by index-matching oil. The illumination can be independently performed with continuous wave white light or a femtosecond laser beam to assess both the scattering and TPL. For the scattering measurements, the sample is illuminated under an incident angle θ by a linearly polarized and collimated white light beam from a 150 W quartz-halogen lamp. The light from the chains is collected by a $\times 40$, 0.65 numerical aperture objective lens in the direction perpendicular to the sample surface and sent to a spectrometer. In order to measure the TPL response of the chains, the white light illumination is replaced by a Kerr-lens mode-locked Ti:sapphire laser which delivers 150 fs pulses at a repetition rate of $f=76$ MHz. The TPL spectrum is obtained by tuning the laser throughout the wavelength range of 685–850 nm. For each incident wavelength, the signal emitted by the chains is collected through the same objective lens as for the scattering experiment and optically filtered through a band-pass filter (BG39, 300–700 nm) before being detected by a photomultiplier tube. A constant power of 15 mW at the prism entrance is ensured by adjusting a neutral density filter. As a last element of our tool box, the Green dyadic formalism[10] is used to compute the complex optical response of the nanochains.

Figure 2(a) shows the scattering spectrum of chains for $N=15$ (N is the number of particles) measured under longitudinal polarization (E field along the chain axis) for both $\theta=0°$ and $\theta=60°$. In agreement with the simulations of Fig. 2(c), a broad scattering band is observed under normal incidence. A sharper peak centered around 718 nm is measured for $\theta=60°$. Its central wavelength gets slightly redshifted to 730 nm when increasing the chain length from $N=15$ to $N=20$. Since this resonance occurs for a similar wavelength than the dipolar resonance of a single particle (around 720 nm), a conventional near-field coupling (where the peak would be strongly redshifted) is excluded. These observa-

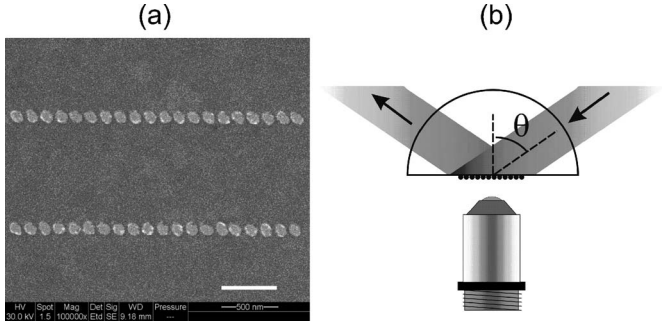

FIG. 1. (a) Scanning electron micrograph of the fabricated gold particle chains (scale bar: 500 nm). (b) Schematic of the optical setup.

[a]Also at: Institute of Space Sciences, Bucharest, Romania.
[b]Also at: ICREA-Institució Catalana de Recerca i Estudis Avançats; electronic mail: romain.quidant@icfo.es

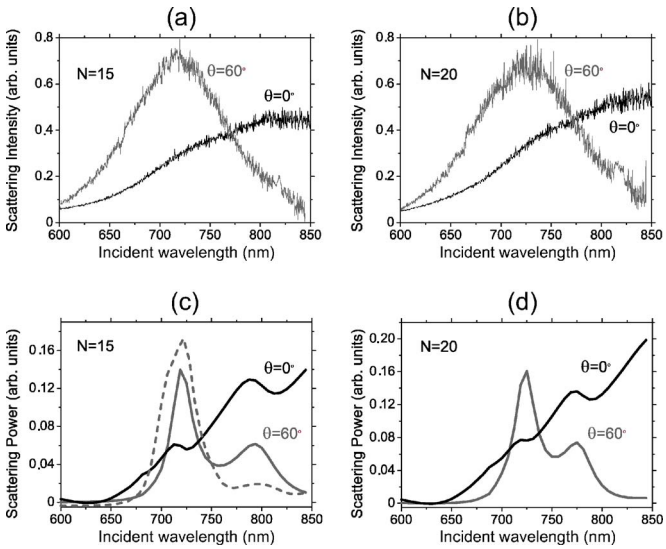

FIG. 2. Experimental scattering intensity spectra for (a) $N=15$ and (b) $N=20$ under $\theta=60°$ (gray) and $\theta=0°$ (black) and longitudinal polarization. [(c) and (d)] Corresponding calculated scattering power spectra. The dashed curve corresponds to an imperfect chains including some geometrical defects.

tions tend to corroborate the existence of resonant modes predicted by the theory, although the double peak features are not resolved by the scattering measurements.

Figures 3(a) and 3(b) show the distribution of the electric near-field intensity computed 20 nm above a 15 particle chain for both $\theta=0°$ and $\theta=60°$ at their respective main scattering resonances. A normalization with the incident intensity at the interface is used. Under total internal reflection (TIR) illumination, one can observe a strong asymmetry of the field along the chain. The intensity increases from the first particle to the last one leading to a high field intensity enhancement at the extremity. This value is more than ten times larger than the maximum intensity observed under normal incidence. At this stage, it is interesting to compare the finite chain geometry to a continuous gold wire with the same section and length. Similar to a chain, calculations for a wire display sharper resonances under TIR illumination compared to normal incidence (data not shown). However, no significant field enhancement occurs for these resonances [Fig. 3(d)]. These data indicate that the in-plane scattering of the particles strongly contributes to the field accumulation at the chain extremity.

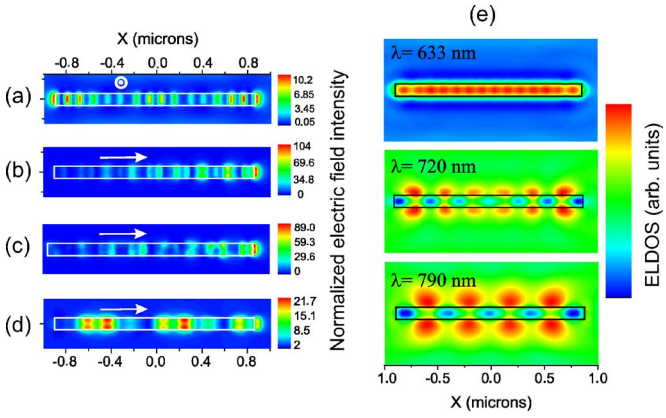

FIG. 3. (Color online) Electric near-field distribution calculated 20 nm above a 15 particle chain for (a) $\theta=0°$ at $\lambda=790$ nm, (b) $\theta=60°$ at $\lambda=720$ nm, (c) $\theta=60°$ at $\lambda=720$ nm for the imperfect chain considered in Fig. 2(c), (d) above a continuous gold wire of the same length and section for $\theta=60°$ at $\lambda=810$ nm. The arrows indicate the incident k vector direction. (e) Evolution with the incident wavelength of the ELDOS calculated 100 nm above a 15 particle chain. The rectangle gives the chain and wire location.

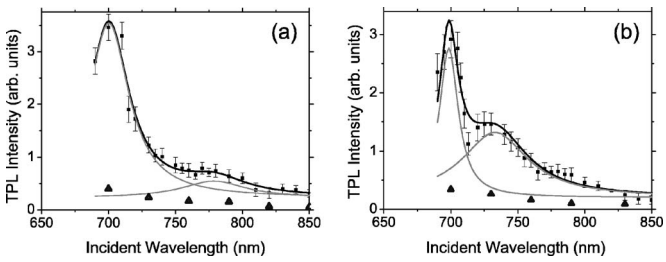

FIG. 4. Evolution of the TPL intensity with the incident wavelength for (a) $N=15$ and (b) $N=20$ both under longitudinal (squares) and transversal (triangles) polarizations. Data points for longitudinal polarization are fitted (red line) with a two peak Lorentzian model.

In order to get further insight into the physical origin of their resonant behavior, we are interested in assessing the intrinsic properties of the chains independently of the illumination and the detection conditions. For this purpose, the local density of electromagnetic states (ELDOS) above the gold particles is computed according to Ref. 11 Figure 3(e) shows the evolution with the incident wavelength of the ELDOS distribution computed 100 nm above a 15 particle chain. Far away from the scattering resonances, at 633 nm, the chain behaves like a discrete object where each of the particles acts individually. Inversely, a clear modulation is observed at $\lambda=720$ nm corresponding to the main resonance of Fig. 2(c). Its period of about 280 nm, different from the pitch of the particles (115 nm), tends to indicate that the chain behaves like a linear cavity where resonances build up from the constructive interference of counterpropagating fields. This hypothesis is confirmed by the lower order resonance (period of 400 nm) observed when switching the incidence to the secondary resonance ($\lambda=790$ nm).

The fact that the double peak is not resolved in the scattering experiment is mainly attributed to the significant background induced both by the detection process and the sample irregularity. For the latest contribution, any defect in the particle shape and dimensions adds a parasite background to the signal associated with the resonant modes of the chains. This is supported by the simulation of Fig. 3(c) (dashed line) performed for an imperfect chain including randomly distributed defect particles with a size deviation of 10%. Although this simple calculation cannot account for the actual degree of imperfections in the fabricated samples, it illustrates the resulting broadening of the resonance peaks in the scattering spectrum. Note that for such imperfect chains, the output field enhancement is maintained significant with a reduction of about 15% [Fig. 3(c)].

Alternatively, nonlinear methods such as TPL have shown to be more suited to assess the local sample properties as the TPL signal is proportional to the fourth power of the electromagnetic field in the metal.[12–14] In the case of resonant plasmon structures where the fields are bound to the metal surface, TPL is expected to be mainly sensitive to the higher field values, thus significantly reducing the background compared to linear techniques.

Figure 4 gives the TPL intensity spectra under TIR illumination ($\theta=60°$) for $N=15$ and $N=20$. In order to check

the reproducibility of the acquired data and rule out any structural modification of the chains induced by the laser illumination,[14] each point of the curves corresponds to an average over two back and forth scans of the laser wavelength. Unlike the experimental scattering curves, the TPL displays a double peak response for both structures as predicted in Figs. 2(c) and 2(d). While the small redshift of the main resonance is not resolved, one can clearly observe the blueshift of the secondary peak. Further discrepancies on the peak position are attributed to the structural differences of the fabricated chains compared to the ideal object considered in the simulation.

Measurements were repeated under transverse polarization (E field perpendicular to the chain axis) to verify that the observed features unambiguously result from modes of the chains. In this case, the TPL intensity remains at a significantly lower value without any peak showing up. Note nevertheless that from the theory a resonance is expected to occur at lower wavelengths (around 680 nm) due to the near-field coupling between the particles. This resonance is weaker compared to the longitudinal polarization and could not be extracted out from the noise level in the scattering experiments but it plausibly explains the slight increase of the TPL signal towards the shortest wavelengths. By calculating the ratio between the maximum TPL intensity under the two polarization states, one can assess the TPL intensity enhancement factor γ associated with the main resonances of Figs. 2(c) and 2(d). We find $\gamma \sim 10$ for the two chain lengths. Although this value indicates higher local field values in the longitudinal polarization state where the cavity modes are expected, it does not permit to deduce the actual enhancement factor of the local field with regard to the incidence. A more direct observation of the spatial field confinement and enhancement at the chain extremity could be done using scanning near-field optical microscopy.

The authors acknowledge the financial support from the NoE "Plasmo-Nano-Devices" (PND)-P6-507 879 and the Spanish government through Grant Nos. TIC2003-01038 and TIC2003-07485 and the program "Ramon-y-Cajal."

[1] J. Kottmann and O. J. F. Martin, Opt. Express **8**, 655 (2001).
[2] K. Li, M. I. Stockman, and D. J. Bergman, Phys. Rev. Lett. **91**, 227402 (2003).
[3] F. H'Dhili, R. Bachelot, G. Lerondel, D. Barchiesi, and P. Royer, Appl. Phys. Lett. **79**, 4019 (2001).
[4] H. Ditbacher, A. Hohenau, D. Wagner, E. Kreibig, M. Rogers, F. Hofer, F. R. Aussenegg, and J. R. Krenn, Phys. Rev. Lett. **95**, 257403 (2006).
[5] H. T. Miyazaki and Y. Kurokawa, Phys. Rev. Lett. **96**, 097401 (2006).
[6] J. R. Krenn, A. Dereux, J. C. Weeber, E. Bourillot, Y. Lacroute, J. P. Goudonnet, G. Schider, W. Gotschy, A. Leitner, F. R. Aussenegg, and C. Girard, Phys. Rev. Lett. **82**, 2590 (1999).
[7] M. Quinten, A. Leitner, J. R. Krenn, and F. R. Aussenegg, Opt. Lett. **23**, 1331 (1998).
[8] S. Maier, P. Kik, H. Atwater, S. Meltzer, E. Harel, B. Koel, and A. Requicha, Nat. Mater. **2**, 229 (2003).
[9] P. Ghenuche, R. Quidant, and G. Badenes, Opt. Lett. **30**, 1882 (2005).
[10] C. Girard and A. Dereux, Rep. Prog. Phys. **59**, 657 (1996).
[11] C. Chicanne, T. David, R. Quidant, J. C. Weeber, Y. Lacroute, E. Bourillot, A. Dereux, G. Colas des Francs, and C. Girard, Phys. Rev. Lett. **88**, 097402 (2002).
[12] P. J. Schuck, D. P. Fromm, A. Sundaramurthy, G. S. Kino, and W. E. Moerner, Phys. Rev. Lett. **94**, 017402 (2005).
[13] P. Muhlschlegel, H. J. Eisler, O. J. F. Martin, B. Hecht, and D. W. Pohl, Science **308**, 1607 (2005).
[14] A. Bouhelier, R. Bachelot, G. Lerondel, G. Kostcheev, P. Royer, and G. P. Wiederrecht, Phys. Rev. Lett. **95**, 267405 (2006).